Indian Journal of Chemical Technology
Vol. 28, September 2021, pp. 595-603

Synthesis of g-carbon nitride-Ag_3PO_4 nanohybrid using Okra plant extract and their photocatalytic activity for the degradation of fluorescein and crystal violet dyes

R Padmanaban & M Dharmendira Kumar*

Department of Applied Sciences and Technology, Alagappa College of Technology, Anna University Chennai 600 025, Tamilnadu, India
E-Mail: mdkumar@annauniv.edu

Received 3 July 2021; accepted 01 September 2021

Development of eco-friendly efficient photo catalyst is an urgent need for waste water treatment in industry. A facile eco-friendly method is established to synthesize hybrid nanocomposite of g-C_3N_4/Ag_3PO_4 using Abelmoschus esculentus plant extract and used as highly efficient photo catalyst for degradation of textile toxins and pharmaceutical waste from industrial waste water. The synthesized catalysts have been characterized by FTIR, XRD, SEM, TEM and EDAX analysis. XRD peaks confirm the cubic phase of Ag_3PO_4, high crystallinity and purity of nanocomposite. SEM studies show nanocomposites with rough surface and irregular morphology. TEM reports confirm the spherical morphology of silver phosphate and it is evenly wrapped on the surface of graphene sheets. EDAX confirms the purity and presence of all elements in composite. Photo catalytic activity of catalyst has been investigated towards degradation of CV and Fluorescein dyes. The superior photo catalytic performance of g-C_3N_4/Ag_3PO_4 nanohybrid composite on CV and Fluorescein dye has been observed and compared with recent report of literature. The photo catalytic studies revealed that the synthesized catalyst is efficient and degrade 95% of Fluorescein and CV within 2 hours. Reusability of the catalyst has been evaluated and it reveals stability and recyclability of the catalyst. The mechanism of photo catalytic activity has also been discussed in detail.

Keywords: g-C_3N_4/Ag_3PO_4, Abelmoschus esculentus, CV, Fluorescein, Nanohybrid

In the past few decades, water pollution is the one of the major global environmental challenges for researchers in developing countries due to growing industries. Even though growing industries is crucial for economic growth of developing countries, it leads to many environmental problems such as environmental pollution, acid rain, climate change etc. As most of the industries discharge hazardous effluents create a threat to the environment and cause severe damage to organisms. Industrial discharge is one of the main causes for environmental damages[1,2]. As the population grows, utilization of pharmaceutical product has been continually growing all over the world. The pollution of pharmaceutical product adversely affects aquatic ecosystems. The presence of medicinally active pharmaceutical metabolite in aquatic environment is to be a serious problem for mankind and surroundings[3-5]. Phenolic compounds are used as raw materials in most of the pharmaceutical and dyeing industries. In addition to the pharmaceutical wastes, discharge of dye effluent from textile dyeing and finishing industries creates huge water pollution and poses potential risk for the human health[6]. CV is a synthetic dye commonly known as Gentian Violet which is a frequently used in pharmaceutical industries as topical antiseptic dye, used for the skin diseases. Fluorescein is another synthetic organic dye which is non-hazardous and widely used as fluorescent tracer for many applications, including mineralogy, gemology, biological detectors etc. CV has been reported as hazardous dye and persist environment for long time and causing for detrimental effect for the environment. As most of the dyes used in industries are toxic and carcinogenic, even the presence of trace amount in waste water is remarkably undesirable for human health[7]. To solve this complication, it is essential to find new methodology or material for removal of toxic contaminants from industrial waste water.

In recent years, Nanotechnology is an emerging and promising technology and has attracted great deal of interest towards the development of nano-based materials such as adsorbents, composites,

semiconductor etc., for water /waste water treatments. Nano structured materials have been emerged and proved as potential candidate for the remediation of hazardous pollutant owing to its large surface volume ratio and their high excellent catalytic activity[8,9]. Heavy metals like Pb, Mo, Cd etc., organic, inorganic pollutants and microbes have been successfully removed by different nano-based materials[10-15]. Most recently graphitic carbon nitride (g-C_3N_4) found to be better photo oxidation performance of synthetic organic dye and effectively degrade Methyl Orange dyes[16,17]. Wang *et al*. also reported that g-C_3N_4, is aconjugative structured, metal free visible light driven semiconductor material with band gap of 2.7 eV and having catalytic ability for evolution of hydrogen from water under visible light irradiation[18-20]. The photo catalytic activity of bare g-C_3N_4 is greatly limited due to rapid recombination of photo generated electron hole pair and large surface area[21,22]. In order to overcome this limitation many attempted have made such as modifying its morphology[23], doping with metals[24] and fabricating composites[25]. However, g-C_3N_4 composite materials can promote its photo catalytic activity by modifying their chemical composition and its structure. Many researchers focused fabricating composites to further improve the photo catalytic activity of bare g-C_3N_4.

Ag_3PO_4 as a photocatalysts has attracted gigantic attention due to its higher visible light activity and has excellent photocatalytic activity with a quantum yield of 90%. Ag_3PO_4 with a band gap of 2.4 eV has exceptionally high photocatalytic efficiency due to its huge potential to avail solar energy. Most recently, Virendrakumar G *et al.* synthesized Ag_3PO_4/g-C_3N_4 composites in various solvent systems and reported the superior catalytic activity of fabricated composites towards the RhB, MB and NP dye pollutants[26]. However, these conventional chemical methods involve some toxic chemical which lead to toxicity and risk to the environment. Moreover, chemically synthesized nanoparticles are not appropriate for medical usage due to presence of some toxic substance that is adsorbed at the surface of the nanoparticles[27]. Therefore, an eco-friendly and economically compatible method is required for the fabrication of Ag_3PO_4/g-C_3N_4 composite.

Recently, Green synthesis is regarded as important tool to reduce the destructive effects associated with chemical synthesis by using mild reaction conditions and nontoxic precursors. Green synthesis of nanoparticles is eco-friendly, time affordable, cost effective and free of hazardous material. Further, medical plants are important sources of biologically active antioxidants and hence extensively studied for green synthesis since they are effective free radical scavengers. *Abelmoschus esculentus* is one of the economically important medical plant and rich in vitamins, minerals and nutrients. Because of high solubility and homogeneous formation, Okra plant extract can be used as reducing agent as well as fuel.

Hence in this work, we synthesized Ag_3PO_4/g-C_3N_4 photo catalyst via eco-friendly route using *Abelmoschus esculentus*, i.e., Okra plant extract. The photo degradation of CV and Fluorescein under visible light irradiation was evaluated to demonstrate the photo catalytic activity of this composite. The effect of various factor on photo catalytic activity and possible mechanism for enhanced activity have been discussed.

Experimental Section

Materials

The leaves of Okra plant were collected from Cuddalore district of Tamilnadu, India. Melamine, silver nitrate ($AgNO_3$) Disodium hydrogen phosphate ($Na_2HPO_4.12H_2O$), Fluorescein and Crystal Violet were purchased from Sigma-Aldrich, India. All the chemicals were AR grade and hence they were used without further purification. DD water was used for preparing solutions.

Preparation of plant extract

Fresh leaves of Okra plant were washed well with fresh water and were dried over sun light. The leaves were grinded by mechanical grinder. 25 g of powder was taken in 100 mL of ethanol and stirred well for half an hour at room temperature. Then it was filtered thoroughly using Whatmann No.1 filter paper. The filtrate was used for the green synthesis.

Synthesis of g-C_3N_4

Graphitic carbon nitride (g-C_3N4) was synthesized by calcination method reported in literature[27]. In a typical synthesis, acid treated melamine was taken in covered alumina crucible and kept in muffle furnace. The sample was initially heated at 250 ·C for one hour, then 350 ·C for another one hour. Heating rate is fixed 5^0C per min continued the heating until reach 550 ·C and maintained at this temperature for 2 h. After completing it, it was allowed to cool at room temperature. The resultant light-yellowcolor sample was named bulky g-C_3N_4. The obtained bulky sample

was immersed in 500 mL deionized water with vigorous stirring and kept under ultra-sonification for10 h. After centrifugation, the obtained g-C_3N_4 nanosheets are used for further characterization.

Synthesis of Ag_3PO_4 nanoparticles

Ag_3PO_4 nanoparticles were prepared by ion exchange method using plant extract[28] and explained through flow chart (Fig. 1). Typically, required quantity of $AgNO_3$ was dissolved in 50 mL of deionized water. Disodium hydrogen phosphate solution was added into it drop by drop with magnetic stirring until the colour changed to yellow. The resultant product washed with water and mixed with 100 mL of plant extract. It was heated to 70 ·C for 5 h in vacuum.

Synthesis of Ag_3PO_4/g-C_3N_4 composite

The schematic illustration of the synthesis of Ag_3PO_4/g-C_3N_4 is shown in Fig. 2. In this synthesis, 50 mg of g-C_3N_4 dispersed into 100 mL of distilled water and ultrasonicated for 10 min. The required amount of synthesized Ag_3PO_4 nano particles were added into it and magnetically stirred for half an hour. 50 mg of PVP was added as surface modifier into the solution and vigorously stirred for several hours. The resultant suspension was introduced into Teflon lined autoclave and continued the heating at 180 ·C for 6 h. The resulting material was heated in a muffle furnace at 300 ·C for 2 h for the complete removal of PVP. The resultant sample was named as Ag_3PO_4/g-C_3N_4 composite.

Characterization techniques

XRD measurements were carried out to analyze the structure nature of the sample using Bruker D8 diffractometerusing Cu-Kα radiation (λ=1.5418 A^0) in the 2-theta range 10 to 80 degree. The distribution morphology of samples was established using Scanning Electron Microscopy (SEM, JEOL Model JSM-6390LV). Microstructure of the composite was analyzed by Transmission Electron Microscope (TEM, H600-II, Hitachi). Elemental composition of composite was determined using Energy dispersive spectra (JEOL model JED-2300). FT-IR, Nicolet Nexus 470 was used to measure the fundamental vibration modes of the samples. For absorption measurement UV-vis-NIR spectrophotometer (Perkin-Elmer lambda 950 was used.

Photo catalytic activity study

The photo catalytic performance of the as prepared different catalyst was evaluated through the degradation of synthetic organic dyes in aqueous solution of different concentrations under different irradiation namely UV, CFL and Visible light. Two different toxic synthetic organic dyes namely, Fluorescein and Crystal violet were chosen to evaluate the photo catalytic activity of the catalyst. In

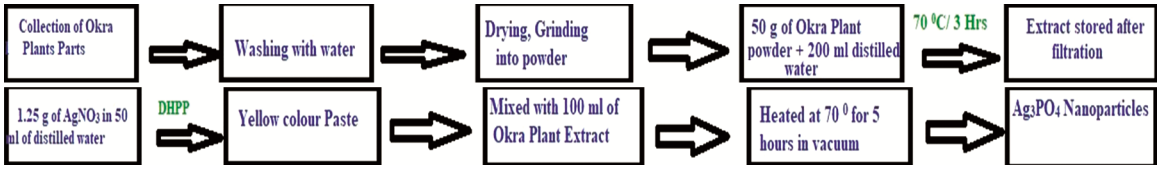

Fig. 1 — Flow chart of green synthesis of Ag_3PO_4 nanoparticles

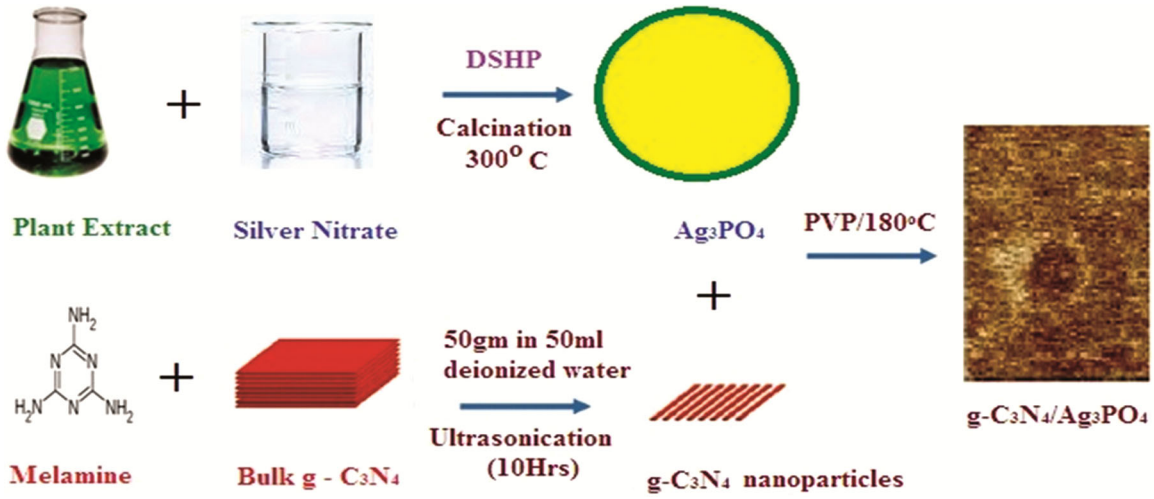

Fig. 2 — Schematic illustration of the synthesis of gC_3N_4/Ag_3PO_4 Composite

a typical procedure, 90 mL of 1×10^{-4} M fluorescein dye solution in DD water was mixed with 10 mL of 1 % wt of catalyst in ethanol with vigorous stirring for one hour for the attainment of perfect adsorption and desorption equilibrium between adsorbent and adsorbate molecules. Then, 20 W UV lamp, Sun light (during noon 11-12), CFL(15 W) were used to irradiate the sample under different condition. 100 ml glass cylinder was used as a batch photo reactor. The corresponding decomposed dye in aqueous solution was taken at specific interval of time and centrifuged to separate the catalyst particle. UV-Vis measurement was performed for the clear solution to determine the absorption maximum in the range of 200-600 nm. All the experiments were performed in triplicate with error below 4% and average values reported. Similar procedure was adopted for CV dye to investigate the degradation efficiency of other catalysts.

Results and Discussion

Powder X-ray diffraction analysis

The XRD analysis was used to determine the structural exactness of components and to analyze the structural crystallinity. The XRD pattern of bare g-C_3N_4, Ag_3PO_4 and g-C_3N_4/Ag_3PO_4 nanocomposite is shown in Fig. 3. In bare g-C_3N_4, two characteristic peaks are observed at $2\theta = 13.1 \cdot$ and $27.5 \cdot$ are indexed to (100) and (002) planes[29]. All the diffraction peaks of Ag_3PO_4 were in good agreement with cubic phase[30,31]. The obtained diffraction peaks are indexed to (200), (210), (211), (310), (222), (320), (321) plane of Ag_3PO_4 [(JCPDS No06-0505) [Ref. 32,33]. No other impurity phases were found in Ag_3PO_4 pattern, suggesting the high purity of the sample. In the XRD

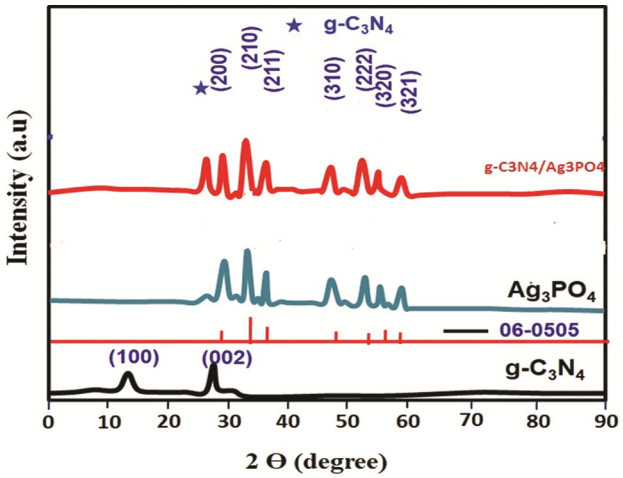

Fig. 3 — XRD pattern of bare gC_3N_4, Ag_3PO_4& gC_3N_4/Ag_3PO_4 Composite

pattern of g-C_3N_4 /Ag_3PO_4 composite, all the diffraction peaks are appeared and suggesting that Ag_3PO_4 loaded on the surface of g-C_3N_4. Debye's Scherer equation was used to calculate the average crystalline size of the samples and the average grain size of g-C_3N_4, Ag_3PO_4 and g-C_3N_4/Ag_3PO_4 were determined from the respective patterns and calculated as 23, 30 and 37 nm, respectively[34].

Morphological analysis

The surface morphology of the sample was examined by SEM, TEM analysis and their results are given in Fig. 4. Figure 4(A) shows that SEM images of synthesized g-C_3N_4 nanoparticles. It exposed the cluster with rough surface and spherical morphology is noted. As observed in the figure all the particles exhibited a porous structure and no obvious agglomerates of g-C_3N_4.The SEM image of Ag_3PO_4 is shown in Fig 4(B) and exposes the spherical structure. Figure 4(C) shows the surface morphology of composite and exposed as irregular morphology. Pristine Ag_3PO_4 catalyst show spherical like morphology with micro sized particles and hence have a tendency for wrapped on graphene sheets. More resolved morphology of the sample studied by TEM and shown in 4(D) and 4(E) and it confirms the independent spherical morphology of Ag_3PO_4 and in the surface of graphene sheets nanoparticle of silver phosphate evenly wrapped. It also suggests the average particle size was around 40 nm for silver phosphate and composite. The particle size agreed with the size calculated through XRD analysis. For the elemental analysis, EDAX of composite material was investigated and report is shown in 4(F) it clearly confirms the presence of major elements Ag, P, O, C, N and also confirm the purity of the sample. The weight percentage and atomic percentage of all the elements are given in Table 1.

FTIR spectra analysis

FTIR analysis revealed characteristic functional groups in g-C_3N_4, Ag_3PO_4 and g-C_3N_4/Ag_3PO_4. Figure 5 indicate FTIR images of g-C_3N_4, Ag_3PO_4 and g-C_3N_4/Ag_3PO_4. The broad peaks appeared at 3000 to 3500 cm^{-1}. It can be attributed by N-H stretching vibration and physically adsorbed water[35]. In case of g-C_3N_4, three types of characteristic vibration mode appeared in the range 1100-1650 cm^{-1} which can be attributed to typical stretching vibration of C-N and C=N in heterocyclic ring[36]. For the composite, two strong peaks appeared at 3205 cm^{-1} and 1665 cm^{-1}

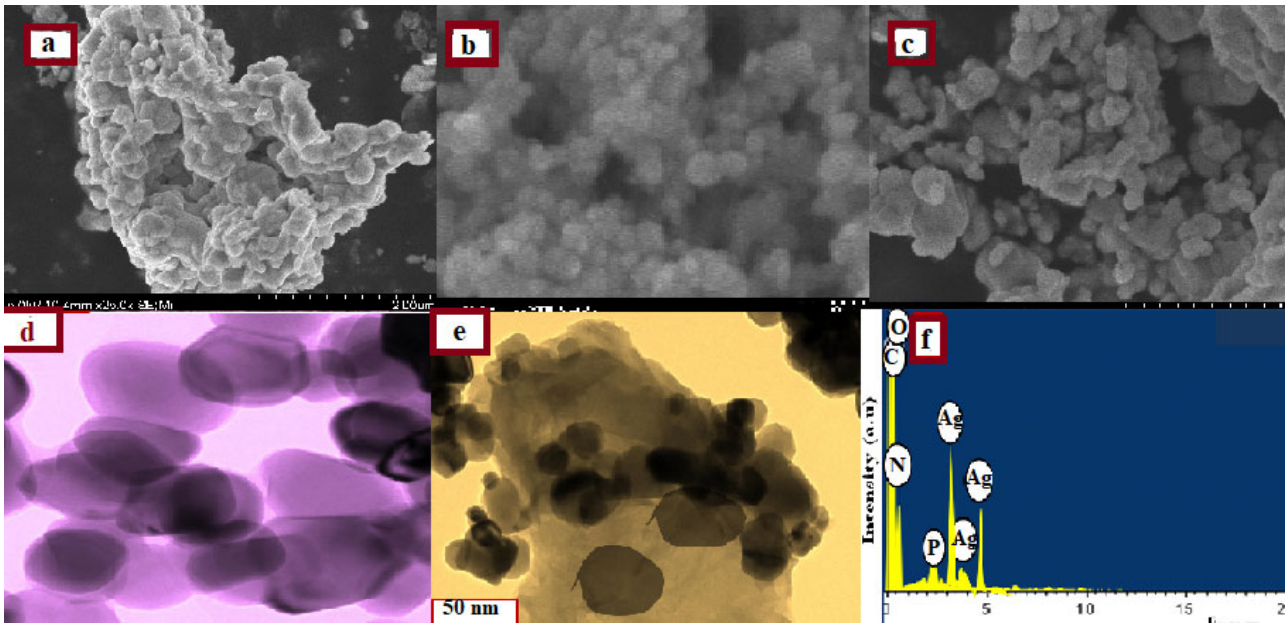

Fig. 4 — SEM images of a) C_3N_4 b) Ag_3PO_4 c) gC_3N_4/Ag_3PO_4 TEM images of d) Ag_3PO_4 e) gC_3N_4/Ag_3PO_4 f)EDAX spectra of gC_3N_4/Ag_3PO_4

Table 1 — EDS elemental quantification results

Element	Weight %	Atomic %
Ag	54.0	65.2
P	7.3	6.1
O	15.7	12.1
C	9.4	7.0
N	13.6	9.6
Total	100	100

which can be attributed to stretching vibration of O-H and bending vibration of O-H in water molecule[37]. For the phosphate group the atomic vibration mode was ascertained at 930 and 545 cm^{-1} [Ref. 38]

Photo catalyticactivity analysis

The procedure of investigation of photo catalytic activity of nanoparticles towards the degradation of synthetic organic dyes are reported in previous work[39]. Photocatalytic efficiency of synthesized g-C_3N_4, Ag_3PO_4 and g-C_3N_4/Ag_3PO_4 composites was evaluated by observing the variation in the λ_{max} value during the photo degradation process. Initially, the photo catalytic activity of the synthesized hybrid composite for degradation of Fluorescein dye was investigated under different irradiation. It illustrates that the UV absorption spectra of Fluorescein irradiated with visible light decreases mostly compared to the other two sources namely, CFL and UV and hence the synthesized hybrid composite is an efficient catalyst for irradiation by solar light.

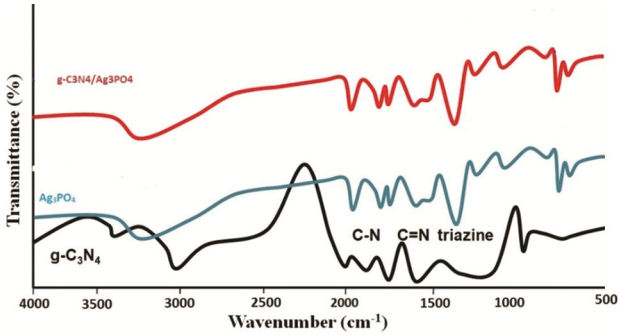

Fig. 5 — FTIR spectra of g-C_3N_4, Ag_3PO_4 and g-C_3N_4/Ag_3PO_4.

Figure 6 a, b and c shows the UV absorption spectra of Fluorescein dye in aqueous solution degraded by g-C_3N_4, Ag_3PO_4 and g-C_3N_4/Ag_3PO_4 catalyst respectively. For the evaluation the photo catalytic efficiency of the catalyst, the characteristic absorption peak at 510 nm was used as reference peak. Moreover, observing corresponding UV absorption peak of Fig 5, the absorption intensity of dye molecule continuously decreases when increasing the irradiation time. The complete disappearance of peak was observed only after 120 min, it suggests the photoactivity of materials and photo degradation increases with increasing the time. It was also confirmed by visually observing colour change of the dye molecule degraded by catalyst in different time interval.

Similarly, the catalytic activity for degradation of CV also evaluated and the resulting UV absorption spectra of CV depicted in Fig.7 a, b and c. Here the

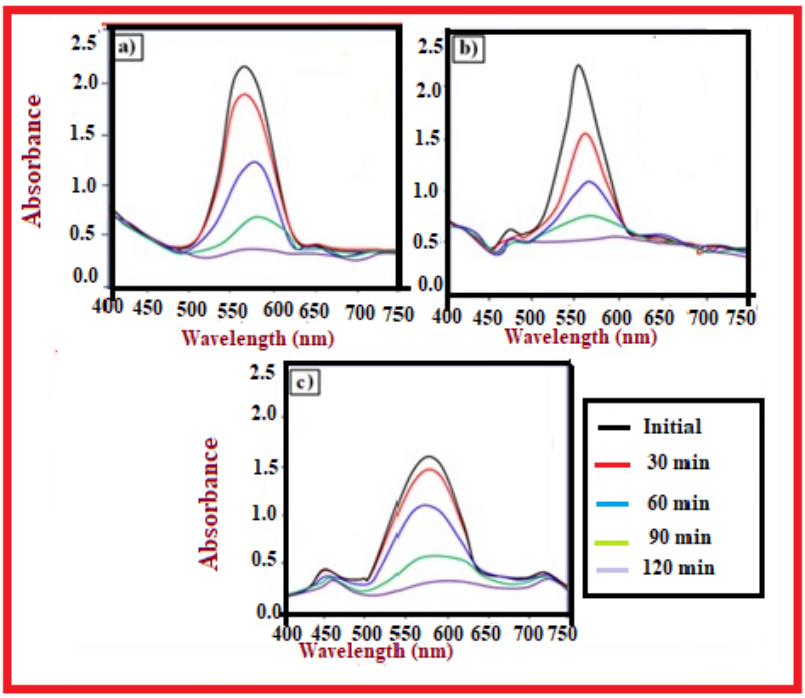

Fig. 6 — Photocatalytic degradation of Fluorescein irradiated by sun light by a) C_3N_4 b) Ag_3PO_4 c) gC_3N_4/Ag_3PO_4

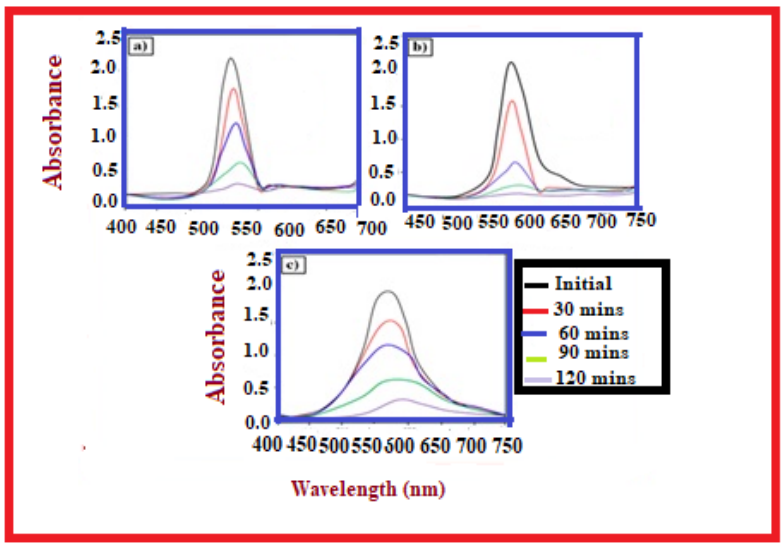

Fig. 7 — Photocatalytic degradation of CV irradiated by sun light by a) C_3N_4 b) Ag_3PO_4 c) gC_3N_4/Ag_3PO_4

characteristic peak at 580 nm was used as reference peak for calculation of efficiency of catalyst. It was also observed that the intensity of absorption peak gradually decreases and hence the synthesized material which is photo active, has the potential to degrade both the dyes.

Kinetic study

The photo catalytic efficiency of the catalyst was calculated from the percentage of degradation of dye molecule under different timings by Langmuir-Hinshelwood equation $\ln(C_0/C) = kt$ [Ref. 40]. The percentage of degradation of Fluorescein and CV is illustrated in Fig. 8a and 8b. It was clearly shown, the degradation % more than 95 % for both dyes in irradiation time of 2 h. The photocatalytic efficiency of the synthesized Ag_3PO_4/gC_3N_4 was compared with the materials synthesized by other methods and listed in Table 2. It can be clearly concluded that the obtained materials by green synthesis have high potential for photocatalytic activity as well as dye removal.

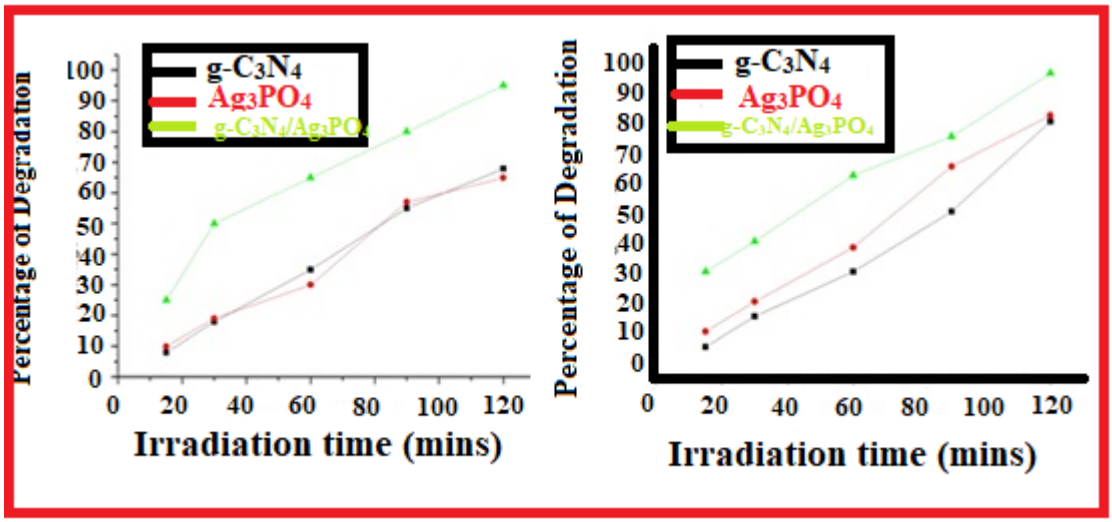

Fig. 8 — Degradation per centage of Fluorescein and CV by gC_3N_4/Ag_3PO_4 under different timings

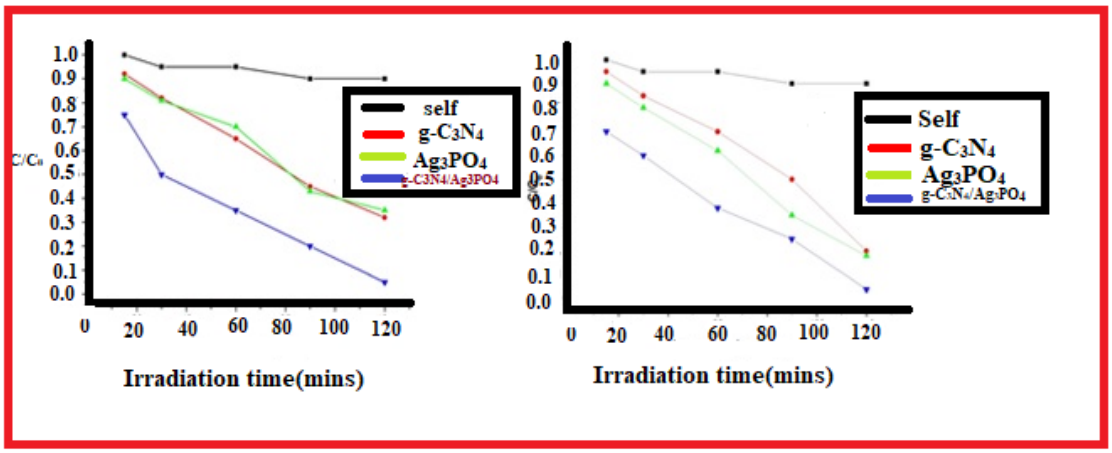

Fig. 9 — Kinetic study of degradation of Fluorescein and CV by gC_3N_4/Ag_3PO_4

Table 2 — Synthetic method and photocatalytic activities of various of gC_3N_4/Ag_3PO_4

Method of synthesis	Dye selected	% Degradation	Reference
Thermal method	RhB	84	[41]
Ultrasonication	RhB and Phenol	90	[42]
Chemical precipitation	Acid Blue 92	89	[43]
Coprecipitation	RhB	88	[44]
Green synthesis using Okra plant extract	Crystal Violet & Fluorescein	>95% for both dyes	-

The kinetic studies were also carried out, and it is depicted in Fig. 9. From the graph it is seen that the absorption intensity increases linearly with concentration and degradation of both dyes follow pseudo first order kinetics.

Reusability study

In order to check the stability of the used catalyst for degradation of dyes, cyclic test was carried out repeatedly using the same catalyst for several times by recovering the catalyst. For the recovery the used catalyst was washed with distilled water and dried at room temperature. The catalytic efficiency of reused catalyst was calculated by comparing it with previous efficiency and results are depicted in Fig. 10. It can be seen that only after 7^{th} experiment, it lost its activity below 90%. Only slight variation was found up to seven experiments; it was more stable catalyst and it can be used for waste water treatment particularly for removal of dyes and heavy metal ions in waste water.

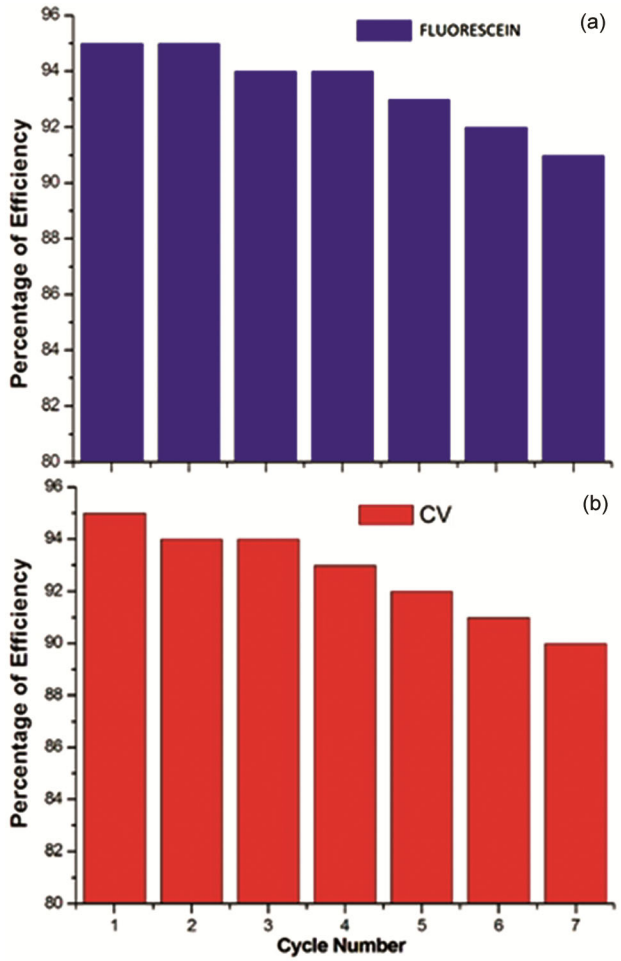

Fig. 10 — Reusability of gC_3N_4/Ag_3PO_4 Photo catalyst for photo degradation of Fluorescein and CV

Photo catalytic mechanism

The photo catalytic mechanism for catalyst irradiated by sun light in the degradation of dye is presented in Fig.11. In general, the mechanism of photo activity of nanomaterial is explained as selective photo oxidation by electron transfer. During the irradiation of visible light, activation of photocatalyst achieved which results in the promotion of electron from VB to CB. The electron transfer continued in efficient manner and reduces the decomposition rate of silver ion in Ag_3PO_4; reduces the rate of catalytic process of Ag_3PO_4. Instantly, diffused photo electron on the surface of Ag_3PO_4 reacts with oxygen molecule in environment to generate reactive species of O^{2-} ions. The generated O^{2-} is transferred to water into hydroxyl radical ($OH^{\cdot}$). The highly reactive species of hydroxyl radical and O^{2-} ions oxidize the dyes into simple product like water and carbon dioxide. As a result, charge separations effectively improved between silver

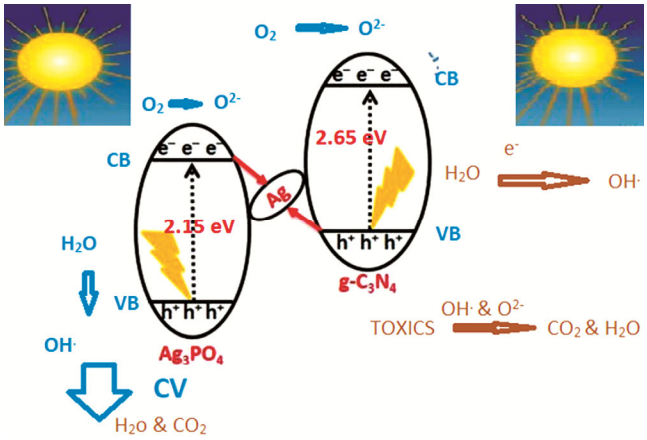

Fig. 11 — Photo catalytic mechanism of degradation on Fluorescein and CV by gC_3N_4/Ag_3PO_4

phosphate and graphitic carbon nitride which enhances the photocatalytic activity.

Conclusion

In summary, this work highlights the green chemistry of synthesizing g-carbon nitride and Ag_3PO_4 nanocomposites from the plant extract of *Abelmoschus esculentus* and developed a new eco-friendly method which is proved to be cost effective, easy and ecofriendly for the synthesis of g-C_3N_4/Ag_3PO_4 nano based hybrid composite using okra plant extract as efficient reducing agent. According to XRD, SEM, TEM, EDAX reports, the presence of both carbon nitrite and Ag_3PO_4 in composite has been confirmed. The hybrid composite show superior photo catalytic activity towards the degradation of Fluorescein and CV dyes compared to their counterpart. The efficiency of the catalyst is compared to already reported activity and reveal significant improvement in their activity. Kinetics of the dye degradation reaction, reusability of the catalyst and mechanism of the improvement activity have also been studied.

Conflict of Interest

The authors declare that there is no conflict of interest.

References

1 Rosenberg N & Birdzell L, "The Rise of the Western WorldNew York", Cambridge University Press, 171 (1973).
2 North D & Thomas R,"How the West Grew Rich: The Economic Transformation of the Industrial World, New York", Basic Books, (1986).
3 Manvendra P, Kumar R, Kishor K, Mlsna T, Pittman C U & Mohan D, *Methods Chem Rev*, 119 (2019) 3510.
4 Ojemaye C Y & Petrik L, *A Review Environ Rev*, 27 (2018) 151.

5 Moon-Kyung Kim & Kyung-Duk Zoh, *Environ Eng Res*, 21 (2016) 319.
6 Chantal Guillard, Lachheb Hinda, Houas Ammar, Ksibi Mohamed, Elaloui Elimame & Jean-Marie Herrmann, *J Photochem Photobiol A: Chem*, 158 (2003) 27.
7 Tim Robinson, McMullan Geoff, Marchant Roger & Nigam Poonam, *Bioresour Technol*, **77** (2001) 247.
8 Pradhan N, Pal A & Pal T, *Langmuir*, 17 (2001) 1800.
9 Sinha A K, Basu M, Sarkar S, Pradhan M & Pal T, *J Colloidal Interface Sci*, 398 (2013) 13.
10 Mir N A, Haque M M, Khan A, Umar K, Muneer M & Vijayalakshmi S, *J Adv Oxid Technol*, 15 (2012) 380.
11 Umar K, Water contamination by organic-pollutants: TiO_2 photocatalysis. In Modern Age Environmental Problems and their Remediation. Springer, Cham, (2018) 95.
12 Kalhapure RS, Sonawane S J & Sikwal D R, *Colloid Surf B*, 136 (2015) 651.
13 Fang X, Li J, Li X, Pan S, Zhang X, Sun X, Han J S W & Wang L, *Chem Eng*, 314 (2017) 38.
14 Sekoai Patrick T, Cecil Naphtaly Moro Ouma, Stephanus Petrus Du Preez, Phillimon Modisha, Nicolaas Engelbrecht, Dmitri G Bessarabov & Anish Ghimire, *Fuel*, 237 (2019) 380.
15 Briggs Andrew M, Marita J Cross, Damian G Hoy, Lidia Sanchez-Riera, Fiona M Blyth, Anthony D Woolf & Lyn March, Gerontologist, 56 (2016) 243.
16 Yan S C, Z S Li & Z G Zou, *Langmuir*, 25 (2009) 10397.
17 Wang X, Chen X, Thomas A, Fu X & Antonietti M, *Adv Mater*, 21 (2009) 1609.
18 Chen Xiufang, Young-Si Jun, Kazuhiro Takanabe, Kazuhiko Maeda, Kazunari Domen, Xianzhi Fu, Markus Antonietti & Xinchen Wang, *Chem Mater*, 21 (2009) 4093.
19 Wang Xinchen, Kazuhiko Maeda, Arne Thomas, Kazuhiro Takanabe, Gang Xin, Johan M, Carlsson, Kazunari Domen & Markus Antonietti, *Nat Mater*, 8 (2009) 76.
20 Maeda K, Wang X, Nishihara Y, Lu D, Antonietti M & Domen K, *J Phys Chem C*, 113 (2009) 4940.
21 Kailasam K, Fischer A, Zhang G, Zhang J, Schwarze M, Schröder M & Thomas A, *Chem Sus Chem*, 8 (2015) 1404.
22 Chai B, Peng T, Mao J, Li K & Zan L, *Phys Chem Chem Phys*, 14 (2012) 16745.
23 Papailias I, Giannakopoulou T, Todorova N, Demotikali D, Vaimakis T & Trapalis C, *Appl Surface Sci*, 358 (2015) 278.
24 Jin Jie, Qian Liang, Chaoying Ding, Zhongyu Li & Song Xu, *J Alloys Comp*, 691 (2017) 763.
25 Xu Difa, Bei Cheng, Weikang Wang, Chuanjia Jiang & Jiaguo Yu, *Applied Catalysis B: Environ*, 231 (2018) 368.
26 Deonikar, Virendrakumar G, Koteshwara Reddy K, Wook-Jin Chung & Hern Kim, J Photochem Photobiol A: Chem, 368 (2019) 168.
27 Upendra Parashar Kumar, Saxena Preeti S & Srivastava Anchal, *Digest J Nanomater Biostruct*, 4 (2009) 159.
28 Yan S C, Li Z S & Zou Z G, Langmuir, 25 (2009) 10397.
29 Huang Kai, Yaohui Lv, Wei Zhang, Shanyun Sun, Bin Yang, Fangli Chi, Songlin Ran & Xianguo Liu, *Mater Res*, 18 (2015) 939.
30 Liao Gaozu, Shuo Chen, Xie Quan, Hongtao Yu & Huimin Zhao, *J Mater Chem*, 22 (2012) 2721.
31 Zhang Xiaojun, Keqiang Yan, Yu Song, Zhe Wang, Jialong Wu & Dayu Yu, *Chem Res Chinese Univ*, 34 (2018) 649.
32 Wang Yunfang, Xiuli Li, Yawen Wang & Caimei Fan, *J Solid State Chem*, 202 (2013) 51.
33 Zhao Yijie, Jing Cao, Haili Lin, Yunjian Wang & Shifu Chen, *Mater Res Bulletin*, 62 (2015) 168.
34 Sivakarthik P, Thangaraj V & Parthibavarman M, *J Mater Sci: Mater Electron*, 28 (2017) 5990.
35 Xu M, Han L & Dong S J, *ACS Appl Mater Interfaces*, 5 (2013) 12533.
36 Yan Jia, Hui Xu, Yuanguo Xu, Cheng Wang, Yanhua Song, Jiexiang Xia & Huaming Li, *J Nanosci Nanotechnol*, 14 (2014) 6809.
37 Zhu Xuewang, Yaxin Shi, Qingzhi Luo, Jing An, Rong Yin, Xueyan Li & Desong Wang, *Mater Res Express*, 612 (2020) 122558.
38 He Yiming, Lihong Zhang, Botao Teng & Maohong Fan, *Environ Sci Technol*, 49 (2015) 649.
39 Sivakarthik P, Thangaraj V, Perumalraj K & Balaji J, *Digest J Nanomater Biostruct*, 11 (2016) 935.
40 Siva Karthik P, Thangaraj V, Kumaresan S & Vallalperuman K, *J Mater Sci: Mater Electron*, 28 (2017) 10582.
41 Deli Jiang, Jianjun Zhu, Min Chen & Jimin Xie, *J Colloid Interface Sci*, 417 (2014) 115.
42 Mingxi Zhang, Hanxiao Du, Juan Ji, Fengfeng Li, Lin Y C, Chenwei Qin, Ze Zhang & Yi Shen, *Molecules*, 26 (2021) 2062.
43 Tasviri M, Armandsefat F, Mohaghegh N & Ahmadinasab N, *Prog React Kinet Mechanism*, 41 (2016) 277.
44 Peizhi He, Limin Song, Shujuan Zhang, Xiaoquing Wu & Qingwu Wei, *Mater Res Bullet*, 51 (2014) 432.